applied sciences

MDPI

Article

The Effect of a Wearable Assistive Trunk Exoskeleton on the Motor Coordination of People with Cerebellar Ataxia

Antonella Tatarelli [1,2], Jan Babič [3], Carlo Casali [4], Stefano Filippo Castiglia [4,5], Giorgia Chini [2], Rosanna Ciancia [6], Ettore Cioffi [1,4], Lorenzo Fiori [2,7], Mariagrazia Michieli [6], Barbara Montante [6], Mariano Serrao [4], Tiwana Varrecchia [2,*] and Alberto Ranavolo [2]

1 Department of Human Neurosciences, Sapienza University of Rome, Viale dell'Università 30, 00185 Rome, Italy; antonellatatarelli@gmail.com (A.T.); ettore.cioffi@uniroma1.it (E.C.)
2 Department of Occupational and Environmental Medicine, Epidemiology and Hygiene, INAIL, Via Fontana Candida, 1, Monte Porzio Catone, 00078 Rome, Italy; g.chini@inail.it (G.C.); lorenzo.fiori@uniroma1.it (L.F.); a.ranavolo@inail.it (A.R.)
3 Laboratory for Neuromechanics and Biorobotics, Department of Automatics, Biocybernetics and Robotics, Jožef Stefan Institute, SI-1000 Ljubljana, Slovenia; jan.babic@ijs.si
4 Department of Medical and Surgical Sciences and Biotechnologies, Sapienza University of Rome, Polo Pontino, Via Franco Faggiana 1668, 04100 Latina, Italy; carlo.casali@uniroma1.it (C.C.); stefanofilippo.castiglia@uniroma1.it (S.F.C.); mariano.serrao@uniroma1.it (M.S.)
5 Department of Brain and Behavioral Sciences, University of Pavia, Via A. Bassi 21, 27100 Pavia, Italy
6 Oncohematology and Cell Therapy Unit, Department of Medical Oncology, CRO Aviano, National Cancer Institute, IRCCS, SI-1000 Ljubljana, Slovenia; rciancia@cro.it (R.C.); mmichieli@cro.it (M.M.); barbara.montante@cro.it (B.M.)
7 Behavioral Neuroscience PhD Program, Department of Physiology and Pharmacology, Sapienza University, Viale dell'Università 30, 00185 Rome, Italy
* Correspondence: t.varrecchia@inail.it

Abstract: The motor features of people with cerebellar ataxia suggest that locomotion is substantially impaired due to incoordination of the head, trunk, and limbs. The purpose of this study was to investigate how well a wearable soft passive exoskeleton worked for motor coordination in these patients. We used an optoelectronic system to examine the gait of nine ataxic people in three different conditions: without an exoskeleton and with two variants of the exoskeleton, one less and the other more flexible. We investigated kinematics using trunk ranges of motion, the displacement of the center of mass in the medio-lateral direction, and the parameters of mechanical energy consumption and recovery. Furthermore, we investigated the lower limb and trunk muscle coactivation. The results revealed a reduction of the medio-lateral sway of the center of mass, a more efficient behavior of the body in the antero-posterior direction, an energy expenditure optimization, a reduction of muscle coactivation and a better coordination between muscle activations. As a result, the findings laid the groundwork for the device to be used in the rehabilitation of individuals with cerebellar ataxia.

Keywords: wearable exoskeleton; exospine; motor coordination; people with cerebellar ataxia

Citation: Tatarelli, A.; Babič, J.; Casali, C.; Castiglia, S.F.; Chini, G.; Ciancia, R.; Cioffi, E.; Fiori, L.; Michieli, M.; Montante, B.; et al. The Effect of a Wearable Assistive Trunk Exoskeleton on the Motor Coordination of People with Cerebellar Ataxia. *Appl. Sci.* **2024**, *14*, 6537. https://doi.org/10.3390/app14156537

Academic Editor: Giuseppe Banfi

Received: 20 June 2024
Revised: 23 July 2024
Accepted: 24 July 2024
Published: 26 July 2024

1. Introduction

The gait of subjects with primary hereditary cerebellar ataxia (swCA) is characterized by abnormalities in all global and segmental gait parameters, leading to an associated high falls risk [1,2] and particularly, increased step width, reduced ankle joint kinematics, increased gait variability, lack of intra-limb and inter-segmental coordination, and reduced trunk control and stability [3–8]. The primary characteristic of the ataxic gait, which has been described regardless of the subtype of CA diagnosis, is the lack of joint coordination, resulting in abnormal coupling of intra-limb joints and upper and lower body segments during walking [1].

SwCA adopt motor strategies that involve the widening of muscle activation timing and increasing the antagonistic muscle coactivation at a single-joint level [9–11] in order to stiffen the body segments, as a strategy to compensate for muscle hypotonia and irregular trajectories [3,12,13]. The trunk plays an important role in these altered movement patterns. Several studies have found increased trunk oscillations which can have a significant impact on stance and gait performance and stability [14–21].

Furthermore, wide upper body oscillations that shift the center of gravity to the borders of the base of support may increase body sway while walking, resulting in the characteristic chaotic gait behavior [22] that exacerbates gait instability and raises the risk of falling [23]. To cope with their walking instability, subjects with cerebellar ataxia adopt motor strategies that involve widening and expanding the muscle activation timing to stiffen body segments [3,14]. However, this compensatory system has some drawbacks, including the possibility of cartilage degradation and increased metabolic costs [24,25].

These findings indicate that it may be appropriate to arrange specific rehabilitation therapy focused on trunk control and/or specific equipment for trunk stabilization during walking [10,14,26,27]. In particular, swCA may benefit from elastic or semirigid orthoses (e.g., elastic suits and/or exoskeletons) that may decrease axis fluctuations in the sagittal and frontal planes without affecting lower limb mobility while walking [7]. Back-support passive exoskeletons have been shown to reduce falls risk and improve trunk stability during gait in healthy subjects [28], as well as constraining trunk movements, which may reduce center of mass (CoM) oscillations and step width and optimize the energetic cost of walking [29–32]. However, the effects of specific assistive devices, particularly elastic or semi-rigid orthoses, on the gait behavior of swCA have not been investigated yet. Reducing trunk oscillations using a passive trunk exoskeleton may help to improve dynamic stability in swCA, resulting in useful tools for supporting the rehabilitation process, reducing falls risk, and assisting swCA in daily activities and work reintegration [33].

Therefore, this pilot study aimed to assess the feasibility of an elastic textile suit equipped with a passive exospine on trunk kinematics, in terms of effectiveness on center of mass behavior and mechanical energy expenditure and recovery, and on lower limb and trunk muscles coactivation during walking in swCA. We considered two passive exospine versions based on energy accumulation and return, one more flexible, MFE, and one less flexible, LFE. This passive exoskeleton presents a mechanical component, the exospine, which was absent in the previous version [28]. We hypothesized that this orthotic device, equipped with a passive exospine, may be effective in supporting the trunks of swCA, helping to reduce oscillations of the trunk and center of mass, and reducing energy expenditure during walking.

2. Materials and Methods

Nine subjects (three females, six males; mean age: 55.4 ± 8.86 years) affected by hereditary degenerative cerebellar ataxia were enrolled in this study. Five were diagnosed with autosomal dominant ataxia (spinocerebellar ataxia [SCA]) while the other four had sporadic adult-onset ataxia (SAOA). We excluded subjects with major involvement of neurological systems other than cerebellar impairment (e.g., extrapyramidal, pyramidal, peripheral nerve, or muscle), as well as those with orthopedic disorders that could cause further gait impairment.

Since swCA may suffer from extracerebellar signs, subjects with gait impairment due to substantial involvement of extracerebellar symptoms, such as pyramidal signs, polyneuropathy, cognitive impairment [MMSE score > 24], oculomotor deficits, and visual abnormalities according to the Snellen visual acuity test, were excluded, as well as those with orthopedic disorders that could cause further gait impairment. We only included swCA who could walk independently and had gait impairments that were solely cerebellar at the time of assessment in a larger group of swCA from a rare disease center.

The Scale for the Assessment and Rating of Ataxia (SARA) was used to assess the disease's characteristics described in Table 1. Seven healthy subjects were enrolled as a

control (C) group (one female, six males; mean age: 58.43 ± 8.6 years). The Declaration of Helsinki was followed by the written informed consent provided by each participant. The local research ethics committee approved the study (CE Lazio 2, protocol number 0139696/2021).

Table 1. Patients' characteristics.

Patients	Age	Gender	Diagnosis	SARA Tot	SARA Gait
P1	67	F	SAOA	18	4
P2	57	F	SAOA	5	2
P3	37	M	SCA1	14	3
P4	54	M	SCA2	14	3
P5	59	M	SAOA	12	3
P6	51	M	SAOA	7	2
P7	66	M	SCA40	6	2
P8	53	F	SCA1	2	1
P9	55	M	SCA1	2	1

2.1. Soft Passive Exoskeleton

A soft passive exoskeleton made of elastic (Lycra) fabric woven with carbon thread was used. The textile module of this exoskeleton has a specific tension and force direction that is useful in ensuring the patient's body alignment in three-dimensional space. These typically extend from the shoulders to the hips, creating a force that opposes trunk movements (Figure 1). The passive exospine designed to be accommodated in the patient's spine using optoelectronic methods [34] is attached to the textile module. Two different versions of the exospine, one more flexible (MFE) and one less flexible (LFE), were used and personalized to subjects' characteristics, fitting perfectly to the posterior surface of the trunk. Because these devices are typically made of shape memory material, they operate on the principle of energy restitution. The MFE and LFE exospines are made up of a sequence of plastic vertebrae and rubber discs (vulkollan 65 shore and 90 shore, respectively) stacked with a pair of harmonic long steel wires with a thickness of 2 mm and 3 mm, respectively (Figures 2 and 3A).

Figure 1. Textile module made of Lycra fabric woven with carbon thread; soft passive exoskeleton.

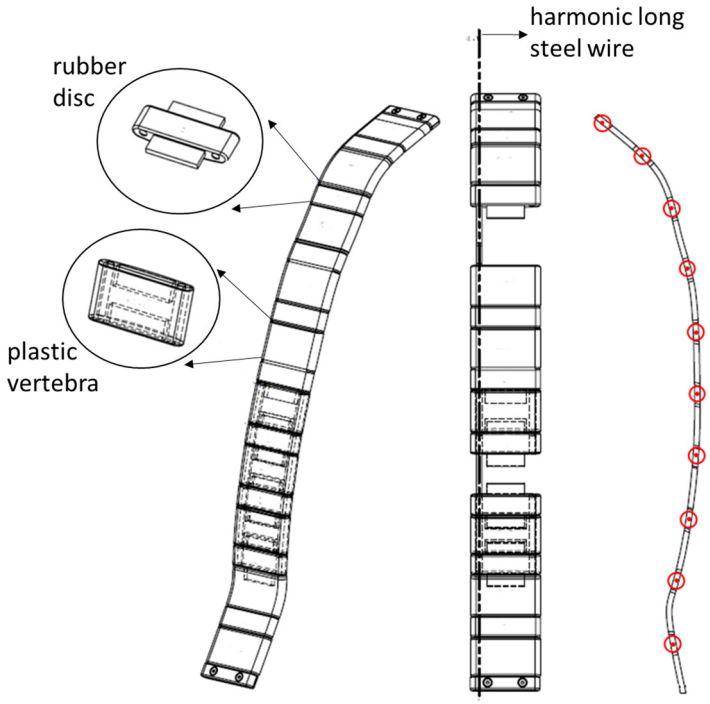

Figure 2. Exospine design with plastic vertebrae, rubber discs, and harmonic long stile wires. Energy storage allows the generation of moments for each element, plastic vertebrae–rubber discs–plastic vertebrae, represented in the figure with red circle (right side).

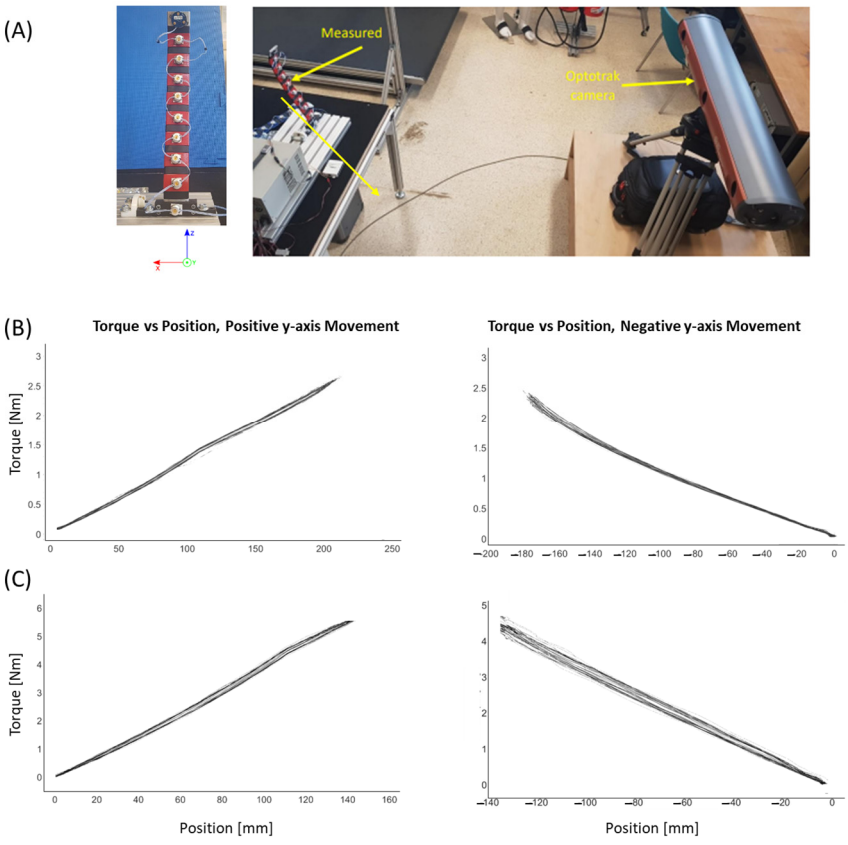

Figure 3. Experimental setup with device position during measurement and corresponding axis of orientation (**A**). Relation between torque and position of topmost vertebrae for more flexible (**B**) and less flexible (**C**) exoskeleton.

Exospines Laboratory Tests

Both exospines were firmly fixed to the table with a 3D printed clamp on their lowest vertebrae. Each vertebra (Figure 3) had a single Optotrak (NDI, Waterloo, ON, Canada) marker on it (3D Accuracy 0.1 mm, resolution 0.01 mm), and only the topmost vertebrae on both devices had an Optotrak marker rig which also enables rotation measurements of the topmost vertebrae. Optotrak camera was placed 2.2 m from the device in positive y-axis (Figure 3A). The force was measured with a beam loadcell TAL220 (SparkFun Electronics, China; 10 kg capacity rating). The loadcell was connected to the top vertebrae with a non-flexible 50 cm long steel wire. Each device has a maximum bend angle which should not be exceeded to prevent irreversible plastic deformation (20° for the MFE and 26° for the LFE from rest position). The loadcell was connected to a multichannel amplifier (Burster 9236, Burster Italia, Curno, Italy), and from there to a NI (Austin, TX, USA) USB 6008 DAC and PC via USB cable. Data were recorded using Simulink (version 7.10.0, MathWorks, Natick, MA, USA). Data from the loadcell and Optotrak were synchronized during measurements. Optotrak has a trigger signal output used, via the NI DAC, as a trigger in Simulink to start recording loadcell data at the same time as the Optotrak system does. The sampling frequency of the loadcell and Optotrak was 100 Hz. The loadcell was calibrated using known weights and, during all measurements, the steel wire was always parallel to the table. Recorded data were filtered using a low-pass 4th order Butterworth filter with a 5 Hz cut-off frequency. Data from loadcell were converted to newtons and torque was calculated as follows:

$$T = Fr \times sin(\vartheta) \quad (1)$$

where r is the level arm and ϑ is the bend angle of the device which should not exceed 20° for the less flexible device and 26° for the more flexible device from rest position to prevent irreversible plastic deformation.

Laboratory tests, with forward (Figure 3B,C left side) and backward (Figure 3B,C right side) movement, have shown that MFE and LFE maximum torque that can be generated during use in sagittal plane is 2.5 Nm (Figure 3B) and 5.5 Nm (Figure 3C), respectively.

2.2. Experimental Procedure

Twenty-six passive markers were tracked by a six-infrared-camera optoelectronic motion analysis system (SMART-DX 6000 System, BTS, Milan, Italy) working at a sampling frequency of 340 Hz. A calibration procedure was executed before the first data-capture was performed, where x is the anterior–posterior, y is the vertical, and z is the medio-lateral direction. Spatial accuracy was 0.2 mm in the x, y, and z dimensions. A global reference system was adopted by the International Society of Biomechanics [35,36]. A modified version of Davis' protocol [37] was used to place the markers (Figure 4) over the spinous processes of the sacrum and seventh cervical vertebra's cutaneous projections and bilaterally over the acromion, elbow, wrist, anterior superior iliac spine, great trochanter, lateral femoral condyle, fibula head, lateral malleoli, heel, and metatarsal head. In addition to markers directly applied to the skin, sticks or wands ranging in length from 7 to 10 cm were placed at 1/3 of the length of the body segment (femur and leg). Anthropometric measurements were taken for each patient after the markers were placed. The gait analysis began with a standing position on a platform. The procedure continued by asking the patient to walk at their preferred speed and in their shoes along a 10 m laboratory pathway on level ground without wearing the device (WOE). Following that, the patients were required to wear the suit, and the exospine was randomly inserted, first in one version and then in the other. For these two conditions, with more flexible (WMFE) and less flexible (WLFE) exospines, the patients were also asked to walk at their preferred speed with their shoes. No external cues were provided during the gait tasks. Healthy subjects were asked to walk at their preferred speed and at a slower but comfortable speed to compare the general characteristics of gait between the groups without any potential bias due to speed differences [38]. In particular, we only took into account trials when the walking speed of each healthy subject fell between the ranges determined by the patients' mean walking

speed plus SD and mean walking speed minus SD [3]. At least ten trials were recorded for ataxic patients in each WOE, WMFE, and WLFE condition and healthy subjects of the control group at each gait speed.

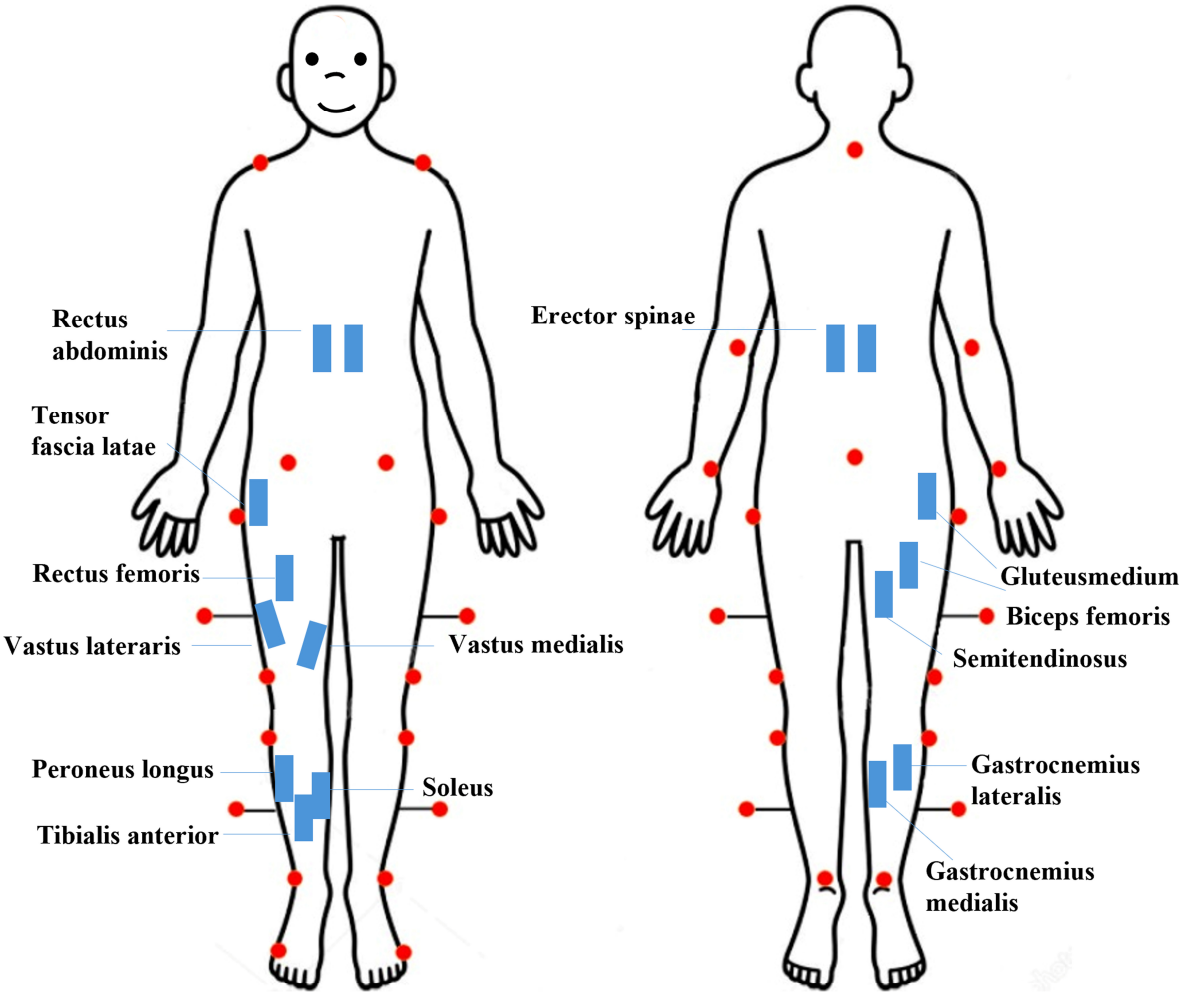

Figure 4. Kinematic (red dots) and surface electromyography (sEMG) protocol.

2.3. Patient Satisfaction Evaluation

Patient satisfaction with the soft passive exoskeleton was assessed using the Quebec User Evaluation of Satisfaction with Assistive Technology (QUEST) [39,40]. The QUEST survey consists of 15 items divided into 2 subscales, allowing patients to rate both the assistive device and the service they received. In our procedure, patients only expressed their satisfaction with the device on a 5-point scale ranging from "very dissatisfied" to "very satisfied". This method aimed to capture patients' perceptions of the usability, comfort, effectiveness, and overall impact that the soft passive exoskeleton could have on their daily activities and quality of life.

2.4. Data Analysis

Marker trajectories were reconstructed using frame-by-frame tracking software (SMART Tracker, BTS, Milan, Italy) following each acquisition performed by Smart Capture (BTS, Milan, Italy). Data processing was conducted using Matlab software (version 7.10.0, MathWorks, Natick, MA, USA) and the SMART Analyzer (BTS, Milan, Italy). The interval between two consecutive foot contacts of the same leg was termed the gait cycle. Using a polynomial technique, kinematic and kinetic data were time-normalized to the duration of the gait cycle and interpolated to 101 samples [41].

2.4.1. Center of Mass Displacement

The whole-body center of mass (CoM) was calculated using the "reconstructed pelvis method" [38,42,43]: the markers over the two anterior superior iliac spines and the sacrum form a triangle, with the geometric center representing the pelvic center. The displacement in medio-lateral direction ($CoM_{displML}$) was then calculated from the CoM as the difference between the maximum and minimum values in medio-lateral direction. The $CoM_{displML}$ was assessed for each condition (WOE, WMFE, WLFE).

2.4.2. Trunk Joint Angles: Range of Motion and Coefficients of Variation

The anatomical joint angles for the trunk (flexion–extension, rotation, and lateral bending) were computed from kinematic data acquired with optoelectronic system. Based on these variables, the joint range of motion (*RoM*) was calculated as the difference between the maximum and minimum values during the gait cycle. The trunk RoMs were assessed for each condition (WOE, WMFE, WLFE).

We calculated the coefficient of variation (*CV*), which is a measure of the variability of a data set (the closer to 0 the *CV* is, the less variable the data), for each *RoM* of trunk joint angles in the sagittal, frontal, and horizontal planes ($CV_{\text{flex-ext}}$, $CV_{\text{lat-ben}}$, and CV_{rot}) as follows [44]:

$$CV = 100 * \frac{SD}{Mean} \tag{2}$$

where, for each parameter, the *Mean* is average across the gait cycles and *SD* is the corresponding standard deviation.

2.4.3. Energy Expenditure Parameters

Mechanical behavior was measured by energy consumption (TEC) [45] and recovery (*R-step*) [46] was computed in relation to the CoM. During the gait cycle, the kinetic energy (E_k) and the potential energy (E_p) associated with CoM displacements were calculated as follows:

$$E_k = E_{kx} + E_{ky} + E_{kz} = \frac{1}{2} m \left(v_x^2 + v_y^2 + v_z^2 \right) \tag{3}$$

$$E_p = mgh \tag{4}$$

where

- m: mass of the CoM;
- E_{kx}, E_{ky} and E_{kz}: kinetic energy on the x, y, and z axes;
- v_x, v_y, and v_z: velocity components of the CoM;
- h: vertical component of the CoM;
- g: acceleration of gravity (m/s^2).

The sum of E_k and E_p was used to calculate the total mechanical energy (E_{tot}) associated with the CoM. The fraction of mechanical energy (*R-step*) recovered during each walking step was calculated as follows [46]:

$$R_{step} = \frac{W_p^+ + W_{kf}^+ - W_{tot}^+}{W_p^+ + W_{kf}^+} \times A = \pi r^2 100 = \left(1 - \frac{W_{tot}^+}{W_p^+ + W_{kf}^+} \right) \times 100 \tag{5}$$

where W_p^+, W_{kf}^+, and W_{tot}^+ represent the positive work produced by gravitational potential energy, forward motion kinetic energy, and total mechanical energy, respectively. The total energy consumption (*TEC*) was then calculated as follows [45]:

$$TEC = \frac{W_{tot}^+}{0.21} \tag{6}$$

The R_{step} and TEC values were averaged for each subject after being normalized to the step length and body weight, respectively. They were assessed for each condition (WOE, WMFE, WLFE).

2.4.4. Electromyographic Data

We used a bipolar 16-channel wireless system (FreeEMG 1000 System, BTS, Milan, Italy) to record sEMG signals at a sample rate of 1000 Hz. Surface electrodes composed of Ag/AgCl were positioned in pairs on the right limb of patients on the gluteus medius, vastus lateralis, vastus medialis, rectus femoris, tensor fascia latae, semitendinosus, biceps femoris, tibialis anterior, gastrocnemius medialis, gastrocnemius lateralis, peroneus longus, soleus, and bilaterally on trunk muscles, abdominis, and erector spinae (Figure 4B), following Atlas of Muscle Innervation Zones [47] and the European Recommendations for Surface Electromyography [48]. To compare strides of varying durations, the sEMG data were time-normalized to the duration of each cycle and reduced to 201 samples using a polynomial procedure [49,50].

2.4.5. Global Muscle Coactivation of Lower Limb and Trunk Muscles

The raw sEMG signals were band-pass filtered (3rd order Butterworth filter at 30–450 Hz), rectified, and low-pass filtered (4th order Butterworth filter with zero lag at 10 Hz). The sEMG signal from each muscle was normalized to its peak median value across all strides and trials for each individual. We assessed the simultaneous activation of 12 lower limb muscles and 4 trunk muscles in each of the three conditions, using the $TMCf$ [51] calculated from the processed sEMG signals:

$$TMCf(d(i),i) = \left(1 - \frac{1}{1+e^{-12(d(i)-0.5)}}\right).\frac{\left(\sum_{m=1}^{M} sEMG_m(i)/M\right)^2}{max_{m=1\ldots M}[sEMG_m(i)]} \quad (7)$$

where M is the number of muscles considered, $EMG_m(i)$ is the $sEMG$ sample value of the mth muscle at instant i, and $d(i)$ is the mean of the differences between each pair among the $sEMG$ signal samples at instant i:

$$d(i) = \left(\frac{\sum_{1}^{M-1}\sum_{m+1}^{M} n\,|sEMG_m(i) - sEMG_n(i)|}{J\left(\frac{M!}{2!(M-2)!}\right)}\right) \quad (8)$$

where $M!/(2!\ (M-2)!)$ represents the total number of possible differences between each pair of sEMG signals and J denotes the signal length (201 samples in this case).

Next, beginning with $TMCf$, we calculated synthetic indices for each condition, including the full width at half maximum ($FWHM_{\text{Trunk}}$ and $FWHM_{\text{limb}}$) that is used to describe the $TMCf$ curves in terms of time amplitude. The $FWHM$ was calculated for each $TMCf$ waveform by adding the durations of the intervals Δt_j in which the $TMCf$ curve exceeded half of its maximum:

$$FWHM = \sum_{j} \Delta t_j \quad (9)$$

Furthermore, for the trunk and lower limb coactivation curves, as well as for each condition (WOE, WMFE, WLFE), we calculated waveform similarity using the coefficient of multiple correlation (CMC): the closer the index is to 1, the more similar the waveforms are [52]. In particular, we calculated the within-subject similarity for $TMCf$ ($CMC_{\text{TMCf\_IS}}$) among all $TMCf$ curves of all strides for each condition, as well as the mean and standard deviation of the $CMC_{\text{TMCf\_IS}}$ across all subjects. The coefficient of multiple correlation was calculated as follows:

$$CMC = \sqrt{1 - \frac{\left(\frac{1}{(T\ (N-1))}\right)\sum_{1}^{N} i\sum_{1}^{T} t\ (y_{it} - \overline{y}_t)^2}{\left(\frac{1}{(T\ N-1)}\right)\sum_{1}^{N} i\sum_{1}^{T} t\ (y_{it} - \overline{y})^2}} \quad (10)$$

where T is the number of time points within the cycle, N represents the curves number, y_{nt} is the value at the t time point in the n_{th} curve, and $\overline{y}_t$ is the average at the time point t over N curves:

$$\overline{y}_t = \frac{1}{N}\sum_{n=1}^{N} y_{nt} \tag{11}$$

where $\overline{y}$ is the grand mean of all y_{nt}:

$$\overline{y} = \frac{1}{NT}\sum_{n=1}^{N}\sum_{t=1}^{T} y_{nt} \tag{12}$$

2.5. Statistical Analysis

Due to the small sample size, to assess the influence of the exoskeleton's presence, a non-parametric Friedman test, which is specific for small samples, was used on each parameter. When significant differences were found, we performed post-hoc analyses. Furthermore, the non-parametric test for comparing small groups, Mann–Whitney test (two-tailed), was used for each parameter to test for between-group differences (WOE vs. C, WMFE vs. C, WLFE vs. C). The same statistical analysis was used to investigate differences in walking speeds between patients in three conditions and between patients and controls. The significance level was set at $p < 0.05$. Matlab software (version 8.3.0.532, MathWorks, Natick, MA, USA) was used for all analyses.

3. Results

No significant differences were found between subjects with cerebellar ataxia and controls age ($p = 0.54$), in the gait speed between subjects with cerebellar ataxia walking in the three conditions (WOE: 0.7 ± 0.05 m/s, WLFE: 0.78 ± 0.12 m/s, WMFE: 0.75 ± 0.07 m/s; $\chi^2 = 0.86$, $p = 0.65$) and between controls (0.79 ± 0.11 m/s) and subjects with cerebellar ataxia (C vs. WOE: $p = 0.066$, C vs. WLFE: $p = 0.36$, C vs. WMFE: $p = 0.2$).

We only reported the results of seven subjects because two patients (P8 and P9 in Table 1), who were in the early stages of the disease, represented outliers compared to the sample.

Table 2 shows the total scores awarded by each subject to both versions of the exoskeleton tested and the mean total scores across all patients.

Table 2. Total QUEST ratings for each patient and both exoskeleton versions utilized.

Patients	P1	P2	P3	P4	P5	P6	P7	Mean ± Std
MFE	3.12	4	4.37	3.5	3.62	4.75	4.5	3.98 ± 0.59
LFE	3.25	4.12	4.62	3.75	4.25	4.25	4.62	4.12 ± 0.48

3.1. Center of Mass Displacement

A statistically significant difference was found for $CoM_{displML}$ between subjects with cerebellar ataxia and control subjects (C vs. WOE, C vs. WLFE, C vs. WMFE: $p < 0.001$) (Figure 5). In both WLFE and WMFE conditions, a statistically significant decrease of the $CoM_{displML}$ was found compared with the condition WOE ($\chi^2 = 8.86$, WOE vs. WMFE: $p = 0.009$, WOE vs. WLFE: $p = 0.03$) (Figure 5) although these oscillations were still significantly higher than those of the control groups.

3.2. Trunk Joint Angles: RoMs and CVs

A significant decrease in trunk flexion–extension and rotation *ROM* values was found in subjects with cerebellar ataxia wearing the LFE compared with the condition WOE ($ROM_{flex\text{-}ext}$, $\chi^2 = 7.75$, WOE vs. WLFE: $p = 0.02$; ROM_{rot}, $\chi^2 = 7.14$, WOE vs. WLFE: $p = 0.02$) (Figure 6).

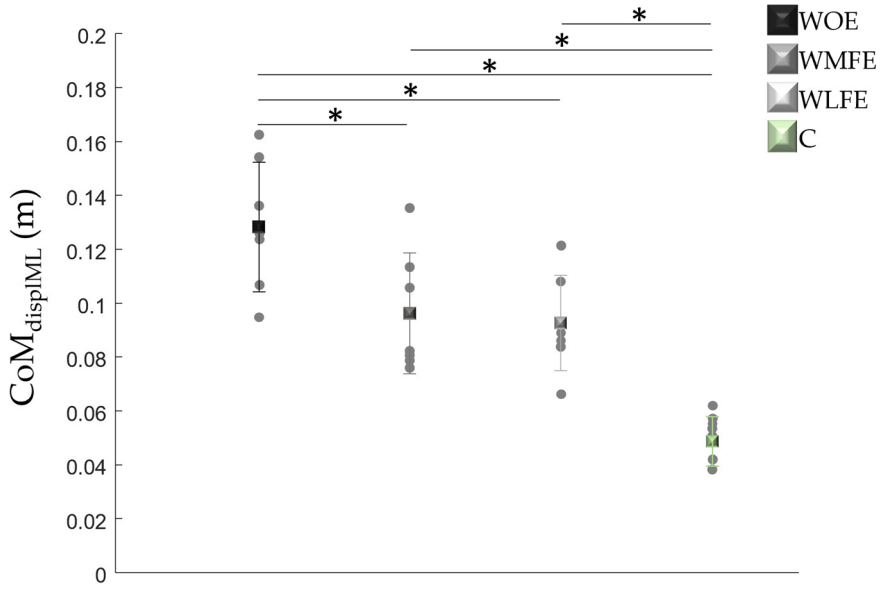

Figure 5. For the patients without the exoskeleton (WOE), with the more (WMFE) and less flexible (WLFE) exoskeleton, and for the control (C) group, the means (±SD) of the displacement of the Center of Mass in the medio-lateral direction (CoM_{dispML}) were reported. Also, in each group, the values of each subject were reported (grey dots). * Statistically significant differences.

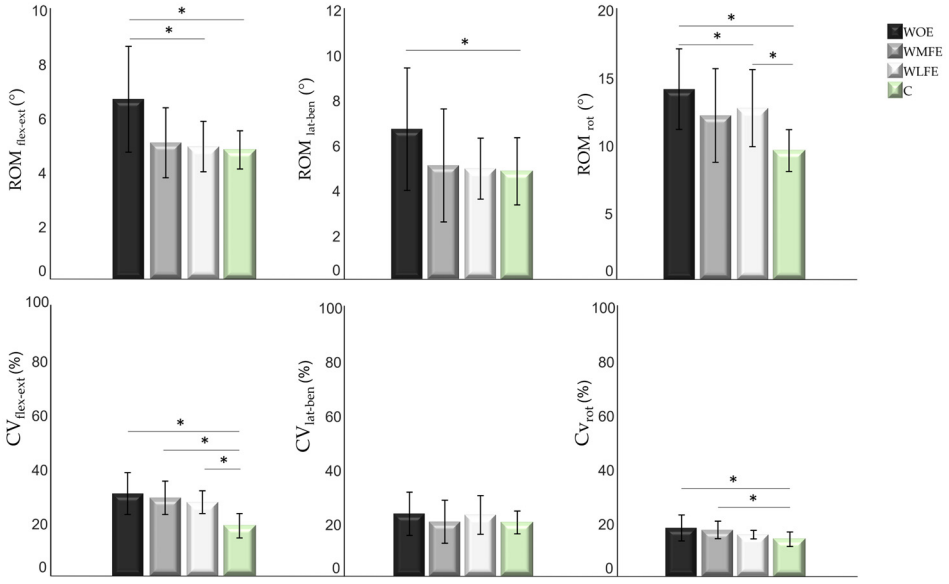

Figure 6. For the patients without the exoskeleton (WOE), with the more (WMFE) and less flexible (WLFE) exoskeleton, and for the control (C) group, the means (±SD) of the range of motion (*RoM*) of trunk flexion–extension, rotation, and lateral bending and coefficients of variation (CVs) of the three RoMs ($CV_{flex-ext}$, CV_{rot}, and $CV_{lat-ben}$) were reported in the first and second row, respectively. * Statistically significant differences.

Furthermore, the values of trunk ROMs calculated without the use of the exoskeleton were significantly higher than those of the control subjects in all three planes of space ($ROM_{flex-ext}$, WOE vs. C: $p = 0.028$; ROM_{rot}, WOE vs. C: $p = 0.002$; $ROM_{lat-ben}$, WOE vs. C: $p = 0.01$).

There was no significant difference between the values of trunk ROMs in the three planes of space in the presence of the exoskeleton and those of the control subjects, except for the trunk rotation *ROM* with the less flexible exoskeleton, which remained significantly higher than the values of healthy subjects (WLFE vs. C: $p = 0.017$) (Figure 6).

The presence of the exoskeleton had no significant effect on the CVs of trunk ROMs; however, a decreasing trend was observed (Figure 6).

Statistical significant differences were found between the values of the CVs of trunk $ROM_{\text{flex-ext}}$ in all three conditions and those of the control subjects (WOE vs. C: $p = 0.006$; WMFE vs. C: $p = 0.01$; WLFE vs. C: $p = 0.003$), and between the values of the CVs of trunk ROM_{rot} WOE and WMFE and those of the control subjects (WOE vs. C: $p < 0.001$; WMFE vs. C: $p = 0.02$). No statistically significant differences were found between the values of the CVs of trunk $ROM_{\text{lat-ben}}$ either between the three conditions or with the control subjects.

3.3. Energy Expenditure Parameters

Statistically significant differences were found for both energetic parameters between ataxic patients and control subjects (*R-step*, C vs. WOE: $p = 0.034$, C vs. WMFE: $p = 0.003$; *TEC*, C vs. WOE: $p = 0.007$). Similarly, a statistically significant increase in *R-step* and decrease in *TEC* were found with the presence of the less flexible exoskeleton compared with the WOE condition (*R-step*, $\chi^2 = 6$, WOE vs. WLFE: $p = 0.04$; *TEC*, $\chi^2 = 6.74$, WOE vs. WLFE: $p = 0.04$) (Figure 7).

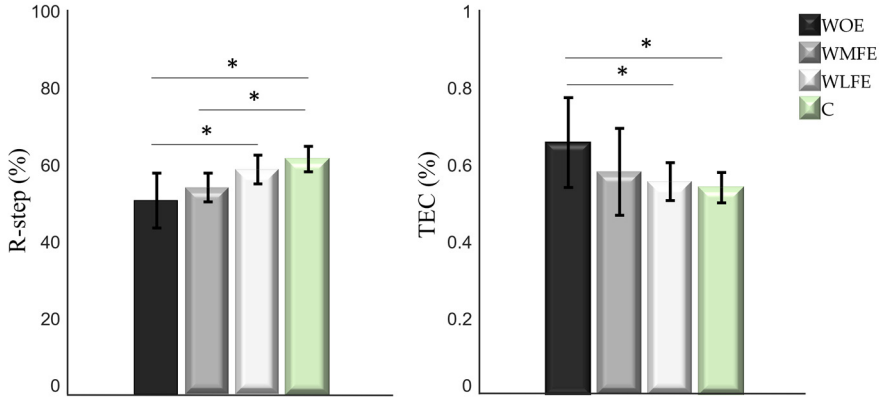

Figure 7. For the patients without the exoskeleton (WOE), with the more (WMFE) and less flexible (WLFE) exoskeleton, and for the control (C) group, the means (±SD) of the recovery (*R-step*) and energy consumption (*TEC*) were reported. * Statistically significant differences.

3.4. Global Muscle Coactivation of Lower Limb and Trunk Muscles

Statistically significant differences were found for both trunk parameters between ataxic patients and control subjects ($FWHM_{\text{Trunk}}$, C vs. WOE: $p < 0.001$, C vs. WMFE: $p = 0.006$, C vs. WLFE: $p = 0.01$; CMC_{Trunk}, C vs. WOE: $p < 0.001$, C vs. WMFE: $p = 0.003$, C vs. WLFE: $p = 0.007$). Furthermore, a statistically significant decrease in $FWHM_{\text{Trunk}}$ was found with the presence of the less flexible exoskeleton compared with the WOE condition ($FWHM_{\text{Trunk}}$, $\chi^2 = 8$, WOE vs. WLFE: $p = 0.03$), and an increase in CMC_{Trunk} was found with the presence of the less flexible exoskeleton compared with the WOE and WMFE conditions (CMC_{Trunk}, $\chi^2 = 5.43$, WOE vs. WLFE: $p = 0.02$, WMFE vs. WLFE: $p = 0.02$) (Figure 8).

Similarly to the trunk, for the lower limbs, statistically significant differences were found for both parameters between ataxic patients and control subjects ($FWHM_{\text{Lower limb}}$, C vs. WOE: $p = 0.001$, C vs. WMFE: $p = 0.02$; $CMC_{\text{Lower limb}}$, C vs. WOE: $p = 0.015$, C vs. WMFE: $p = 0.04$). Statistically significant decreases in $FWHM_{\text{Lower limb}}$ and increases in $CMC_{\text{LowerLimb}}$ were found with the presence of the less flexible exoskeleton compared with the WOE condition ($FWHM_{\text{Lower limb}}$, $\chi^2 = 8.86$, WOE vs. WLFE: $p = 0.04$; $CMC_{\text{Lower limb}}$, $\chi^2 = 8.22$, WOE vs. WLFE: $p = 0.007$) (Figure 9).

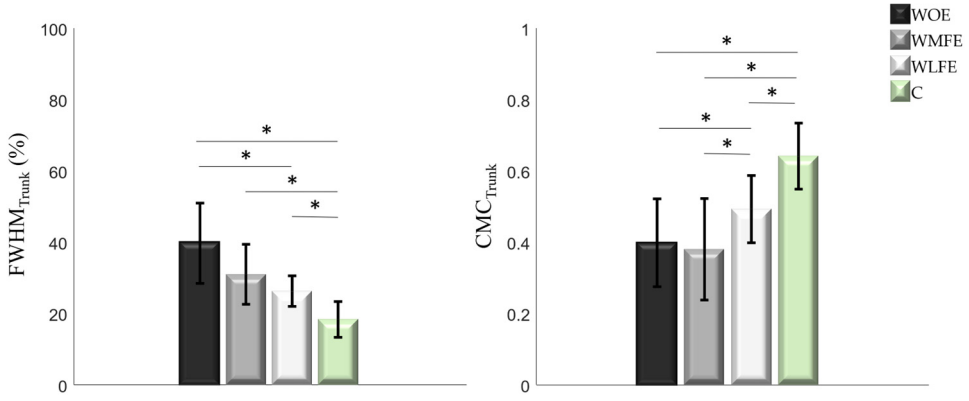

Figure 8. For the patients without the exoskeleton (WOE), with the more (WMFE) and less flexible (WLFE) exoskeleton, and for the control (C) group, the means (±SD) of the full width at half maximum ($FWHM_{Trunk}$) and intrasubject coefficient of multiple correlation (CMC_{Trunk}) for trunk were reported. * Statistically significant differences.

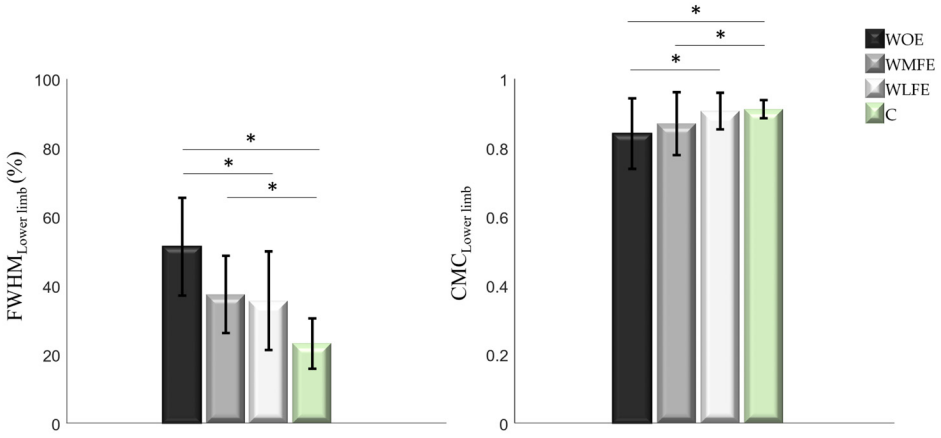

Figure 9. For the patients without the exoskeleton (WOE), with the more (WMFE) and less flexible (WLFE) exoskeleton, and for the control (C) group, the means (±SD) of the full width at half maximum ($FWHM_{Lower\ limb}$) and intrasubject coefficient of multiple correlation ($CMC_{Lower\ limb}$) for the lower limbs were reported. * Statistically significant differences.

4. Discussion

The aim of this pilot study was to investigate the feasibility of using an elastic textile suit equipped with two passive exospines, one more and one less flexible, in terms of effects on trunk kinematics, center of mass behavior, and mechanical energy expenditure and recovery during walking.

We found that CoM displacement reduced when using the exospine, compared to walking without the device, regardless of the flexibility of the exoskeleton. Moreover, we found that trunk RoMs in the frontal and transverse planes reduced in swCA when using the less flexible exoskeleton. Reducing body sway and trunk oscillations is an important rehabilitation target in swCA [26,27], and our results are consistent with the findings by Serrao et al., who found a reduction of medio-lateral body sway and pelvic oscillations when swCA [14] wore a dynamic movement orthosis. Moreover, we found that the WLFE condition reduced the variability of trunk rotation. However, our sample was too small to reach consistent results in terms of correlations between the improvements in trunk range of motion and CoM displacement; therefore, this mechanism deserves to be better investigated on larger samples, particularly when wearing the less flexible configuration.

We also found that *R-Step* increased and TEC was reduced when swCA wore the less flexible exoskeleton. *R-Step* measures the efficiency in recovering mechanical energy during the gait cycle, whereas TEC is a measure of mechanical energy consumption [45,46].

Our findings are consistent with the operating principle of the exoskeleton, which is based on the ability to store energy during the load acceptance phase and return it during the propulsion phase, allowing the patient exoskeleton system to store and reuse kinetic energy more efficiently. This is further confirmed by the results of sEMG analysis, showing a reduction in *FWHM* and increase in *CMC* values for both the lower limb and trunk muscles when wearing the less flexible exoskeleton. SwCA have been described to increase muscle coactivation as a global compensatory mechanism to deal with the enlarged lateral body sway caused by a lack of inter-joint coordination and hypotonia, which impairs their ability to recover energy while walking. In this way, it is possible to argue that using the less flexible exoskeleton, by allowing a more efficient walking behavior and reducing CoM displacement, reduces the need for swCA to increase the muscle coactivation and allows a better coordination between muscle activations, as expressed by *CMC* values.

This increased capacity for mechanical energy management may explain the improved behavior in the sagittal plane with the consequent reduction of spurious oscillations on the frontal plane. With each step cycle with the exoskeleton, a higher part of the CoM kinetic energy is converted into gravitational potential energy and then back into kinetic energy. In this case, the locomotory muscles must supply a lower power to overcome the losses occurring during the energy transduction required to move the CoM [45]. This is further confirmed by the results of sEMG analysis, showing a reduction in *FWHM* and an increase in *CMC* values for both the lower limb and trunk muscles when wearing the less flexible exoskeleton. SwCA have been described to increase muscle coactivation as a global compensatory mechanism to deal with the enlarged lateral body sway caused by a lack of inter-joint coordination and hypotonia, which impairs their ability to recover energy while walking [11]. In this way, it is possible to argue that using the less flexible exoskeleton, by allowing a more efficient walking behavior and reducing CoM displacement, reduces the need for swCA to increase the muscle coactivation and allows better coordination between muscle activations, as expressed by *CMC* values.

Another datum that well explains the effectiveness of the device is associated with the reduction of the variability monitored in the conditions of use of the exoskeleton compared to that of non-use. The increased variability between gait cycles is a typical characteristic of ataxic patients [53] and having the possibility of reducing it means offering them the possibility of moving in three-dimensional space more efficiently and safely.

As this was a pilot study, no sample size analysis was performed prior to recruitment. This represents a limitation of this study, together with the small sample size. In this way, the results of this study should be interpreted cautiously. However, the findings of this study may allow us to conduct further studies with larger samples, and also to analyze any differences in gender and decades of age. It will also be necessary to analyze the behavior of the forces exchanged with the environment. This also allows us to better understand the strategies adopted by the central nervous system in managing the interaction with the exoskeleton.

Another limitation of this study is that we only examined the gait of swCA who could walk independently, excluding subjects with a more severe disability, to which our findings cannot be directly applied. Furthermore, we were unable to conduct subgroup analysis to highlight differences between types of degenerative CA, and we only evaluated subjects with inherited degenerative CA, ruling out subjects with other cerebellar disorders. Furthermore, we only investigated linear walking in the steady state. Although walking on a 10 m walkway may be sufficient to assess the walking capacity of swCA [54,55], they also experience dynamic unbalance during transitions or externally perturbed conditions. Therefore, additional studies should be conducted to explore the effects of the device during more demanding locomotor tasks such as curvilinear and tandem walking, gait initiation and termination, etc. [56]

Further studies will also be necessary for medium- and long-term evaluations of wearing these devices for long periods, to also evaluate thermal comfort through the use of

a thermal manikin, and to analyze confounding factors which would have been possible if we had also investigated the walking of the control subjects wearing the exoskeleton.

5. Conclusions

The results of our study revealed a reduction of the medio-lateral sway of the center of mass, a more efficient behavior of the body in the antero–posterior direction, an energy expenditure optimization, a reduction of muscle coactivation, and a better coordination between muscle activations of individuals with cerebellar ataxia wearing the exoskeleton. These findings encourage the use of passive assistive devices based on the principle of energy accumulation and return to normalize trunk behavior during walking in patients with cerebellar ataxia. These trunk aids promote better management of mechanical energy.

Author Contributions: Conceptualization, A.R., A.T., B.M., R.C., M.M. and M.S.; methodology, A.T., J.B., G.C., E.C., L.F., T.V. and A.R.; validation, A.R. and J.B.; formal analysis, A.T., J.B., G.C., E.C., L.F., B.M. and T.V.; investigation, A.T., J.B., G.C., E.C., L.F., S.F.C., B.M. and T.V.; writing—original draft preparation, A.T., G.C., A.R. and T.V.; writing—review and editing, A.T., J.B., C.C., S.F.C., G.C., R.C., E.C., L.F., B.M., M.M., M.S., T.V. and A.R.; supervision, A.R. and M.S.; project administration, A.R. and M.M.; funding acquisition, A.R., R.C., B.M. and M.M. All authors have read and agreed to the published version of the manuscript.

Funding: This research was funded by Friuli Venezia Giulia POR FESR 2014-2020, Activity 1.3.b—DGR 1489/2017, grant number 8981/LAVFORU 11 October 2018.

Institutional Review Board Statement: The study was conducted in accordance with the Declaration of Helsinki and approved by the local research ethics committee (CE Lazio 2, protocol number 0139696/2021).

Informed Consent Statement: Informed consent was obtained from all subjects involved in the study.

Data Availability Statement: Dataset available on request from the authors.

Acknowledgments: We thank Stefano Pezzutti and Paolo Sacilotto of Latofres srl and Nello Cividino and Enrico Cividino of Porzio for the administrative and technical support provided throughout the project.

Conflicts of Interest: The authors declare no conflicts of interest.

References

1. Jin, L.; Lv, W.; Han, G.; Ni, L.; Sun, D.; Hu, X.; Cai, H. Gait characteristics and clinical relevance of hereditary spinocerebellar ataxia on deep learning. *Artif. Intell. Med.* **2020**, *103*, 101794. [CrossRef] [PubMed]
2. Buckley, E.; Mazzà, C.; McNeill, A. A systematic review of the gait characteristics associated with Cerebellar Ataxia. *Gait Posture* **2018**, *60*, 154–163. [CrossRef] [PubMed]
3. Mari, S.; Serrao, M.; Casali, C.; Conte, C.; Martino, G.; Ranavolo, A.; Coppola, G.; Draicchio, F.; Padua, L.; Sandrini, G.; et al. Lower limb antagonist muscle co-activation and its relationship with gait parameters in cerebellar ataxia. *Cerebellum* **2014**, *13*, 226–236. [CrossRef] [PubMed]
4. Palliyath, S.; Hallett, M.; Thomas, S.L.; Lebiedowska, M.K. Gait in patients with cerebellar ataxia. *Mov. Disord.* **1998**, *13*, 958–964. [CrossRef] [PubMed]
5. Ilg, W.; Golla, H.; Thier, P.; Giese, M.A. Specific influences of cerebellar dysfunctions on gait. *Brain* **2007**, *130*, 786–798. [CrossRef] [PubMed]
6. Cabaraux, P.; Gandini, J.; Kakei, S.; Manto, M.; Mitoma, H.; Tanaka, H. Dysmetria and errors in predictions: The role of internal forward model. *Int. J. Mol. Sci.* **2020**, *21*, 6900. [CrossRef] [PubMed]
7. Manto, M. Cerebellar motor syndrome from children to the elderly. *Handb. Clin. Neurol.* **2018**, *154*, 151–166. [PubMed]
8. Manto, M.; Huisman, T.A. *The Cerebellum: Disorders and Treatment: Handbook of Clinical Neurology Series*; Elsevier: Amsterdam, The Netherlands, 2018.
9. Morton, S.M.; Bastian, A.J. Cerebellar control of balance and locomotion. *Neuroscientist* **2004**, *10*, 247–259. [CrossRef] [PubMed]
10. Ilg, W.; Timmann, D. Gait ataxia—Specific cerebellar influences and their rehabilitation. *Mov. Disord.* **2013**, *28*, 1566–1575. [CrossRef]
11. Fiori, L.; Ranavolo, A.; Varrecchia, T.; Tatarelli, A.; Conte, C.; Draicchio, F.; Castiglia, S.F.; Coppola, G.; Casali, C.; Pierelli, F.; et al. Impairment of global lower limb muscle coactivation during walking in cerebellar ataxias. *Cerebellum* **2020**, *19*, 583–596. [CrossRef]

12. Bodranghien, F.; Bastian, A.; Casali, C.; Hallett, M.; Louis, E.D.; Manto, M.; Mariën, P.; Nowak, D.A.; Schmahmann, J.D.; Serrao, M.; et al. Consensus paper: Revisiting the symptoms and signs of cerebellar syndrome. *Cerebellum* **2016**, *15*, 369–391. [CrossRef] [PubMed]
13. Marchese, S.M.; Farinelli, V.; Bolzoni, F.; Esposti, R.; Cavallari, P. Overview of the Cerebellar Function in Anticipatory Postural Adjustments and of the Compensatory Mechanisms Developing in Neural Dysfunctions. *Appl. Sci.* **2020**, *10*, 5088. [CrossRef]
14. Serrao, M.; Casali, C.; Ranavolo, A.; Mari, S.; Conte, C.; Chini, G.; Leonardi, L.; Coppola, G.; Di Lorenzo, C.; Harfoush, M.; et al. Use of dynamic movement orthoses to improve gait stability and trunk control in ataxic patients. *Eur. J. Phys. Rehabil. Med.* **2017**, *53*, 735–743. [CrossRef] [PubMed]
15. Horak, F.B.; Diener, H.C. Cerebellar control of postural scaling and central set-in stance. *J. Neurophysiol.* **1994**, *72*, 479–493. [CrossRef] [PubMed]
16. Holmes, G. The cerebellum of man. *Brain* **1939**, *62*, 1–30. [CrossRef]
17. Hallett, M.; Massaquoi, S.G. Physiologic studies of dysmetria in patients with cerebellar deficits. *CJNS* **1993**, *20*, S83–S92.
18. Diener, H.C.; Dichgans, J. Cerebellar and spinocerebellar gait disorders. In *Woollacott Clinical Disorders of Posture and Gait*; Bronstein, A.M., Brandt, T., Eds.; CRC Press: London, UK, 1996; pp. 147–155.
19. Konczak, J.; Timmann, D. The effect of damage to the cerebellum on sensorimotor and cognitive function in children and adolescents. *Neurosci. Biobehav. Rev.* **2007**, *31*, 1101–1113. [CrossRef] [PubMed]
20. Bastian, A.J. Moving, sensing and learning with cerebellar damage. *Curr. Opin. Neurobiol.* **2011**, *21*, 596–601. [CrossRef] [PubMed]
21. Goodworth, A.D.; Paquette, C.; Jones, G.M.; Block, E.W.; Fletcher, W.A.; Hu, B.; Horak, F.B. Linear and an-gular control of circular walking in healthy older adults and subjects with cerebellar ataxia. *Exp. Brain Res.* **2012**, *219*, 151–161. [CrossRef] [PubMed]
22. Earhart, G.M.; Bastian, A.J. Selection and coordination of human locomotor forms following cerebellar damage. *J. Neurophysiol.* **2001**, *85*, 759–769. [CrossRef]
23. Schniepp, R.; Schlick, C.; Pradhan, C.; Dieterich, M.; Brandt, T.; Jahn, K.; Wuehr, M. The interrelationship between disease severity, dynamic stability, and falls in cerebellar ataxia. *J. Neurol.* **2016**, *263*, 1409–1417. [CrossRef]
24. Peterson, D.S.; Martin, P.E. Effects of age and walking speed on coactivation and cost of walking in healthy adults. *Gait Posture* **2010**, *31*, 355–359. [CrossRef]
25. Griffin, T.M.; Guilak, F. The role of mechanical loading in the onset and progression of osteoarthritis. *Exerc. Sport. Sci. Rev.* **2005**, *33*, 195–200. [CrossRef] [PubMed]
26. Miyai, I.; Ito, M.; Hattori, N.; Mihara, M.; Hatakenaka, M.; Yagura, H.; Sobue, G.; Nishizawa, M. Cerebellar ataxia rehabilitation trial in degenerative cerebellar diseases. *Neurorehabilit. Neural Repair* **2012**, *26*, 515–522. [CrossRef]
27. Ilg, W.; Synofzik, M.; Brotz, D.; Burkard, S.; Giese, M.A.; Schols, L. Intensive coordinative training improves motor performance in degenerative cerebellar disease. *Neurology* **2009**, *73*, 1823–1830. [CrossRef] [PubMed]
28. Park, J.H.; Kim, S.; Nussbaum, M.A.; Srinivasan, D. Effects of back-support exoskeleton use on gait performance and stability during level walking. *Gait Posture* **2022**, *92*, 181–190. [CrossRef] [PubMed]
29. Arvin, M.; van Dieën, J.H.; Bruijn, S.M. Effects of constrained trunk movement on frontal plane gait kinematics. *J. Biomech.* **2016**, *13*, 3085–3089. [CrossRef] [PubMed]
30. Park, J.H.; Lee, Y.; Madinei, S.; Kim, S.; Nussbaum, M.A.; Srinivasan, D. Effects of Back-Support Exoskeleton Use on Lower Limb Joint Kinematics and Kinetics During Level Walking. *Ann. Biomed. Eng.* **2022**, *50*, 964–977. [CrossRef]
31. Ijmker, T.; Houdijk, H.; Lamoth, C.J.; Beek, P.J.; van der Woude, L.H. Energy cost of balance control during walking decreases with external stabilizer stiffness independent of walking speed. *J. Biomech.* **2013**, *46*, 2109–2114. [CrossRef] [PubMed]
32. Del Ferraro, S.; Falcone, T.; Ranavolo, A.; Molinaro, V. The Effects of Upper-Body Exoskeletons on Human Metabolic Cost and Thermal Response during Work Tasks—A Systematic Review. *Int. J. Environ. Res. Public Health* **2020**, *17*, 7374. [CrossRef]
33. Ranavolo, A.; Serrao, M.; Varrecchia, T.; Casali, C.; Filla, A.; Roca, A.; Silvetti, A.; Marcotulli, C.; Rondinone, B.M.; Iavicoli, S.; et al. The Working Life of People with Degenerative Cerebellar Ataxia. *Cerebellum* **2019**, *18*, 910–921. [CrossRef] [PubMed]
34. Ranavolo, A.; Don, R.; Draicchio, F.; Bartolo, M.; Serrao, M.; Padua, L.; Cipolla, G.; Pierelli, F.; Iavicoli, S.; Sandrini, G. Modelling the spine as a deformable body: Feasibility of reconstruction using an optoelectronic system. *Appl. Ergon.* **2013**, *44*, 192–199. [CrossRef] [PubMed]
35. Wu, G.; Siegler, S.; Allard, P.; Kirtley, C.; Leardini, A.; Rosenbaum, D.; Whittle, M.; D D'Lima, D.; Cristofolini, L.; Witte, H.; et al. ISB recommendation on definitions of joint coordinate system of various joints for the reporting of human joint? motion—Part I: Ankle, hip, and spine. International Society of Biomechanics. *J. Biomech.* **2002**, *35*, 543–548. [CrossRef]
36. Wu, G.; van der Helm, F.C.; Veeger, H.E.; Makhsous, M.; Van Roy, P.; Anglin, C.; Nagels, J.; Karduna, A.R.; McQuade, K.; Wang, X.; et al. ISB recommendation on definitions of joint coordinate systems of various joints for the reporting of human joint motion—Part II: Shoulder, elbow, wrist and hand. *J. Biomech.* **2005**, *38*, 981–992. [CrossRef] [PubMed]
37. Tatarelli, A.; Serrao, M.; Varrecchia, T.; Fiori, L.; Draicchio, F.; Silvetti, A.; Conforto, S.; De Marchis, C.; Ranavolo, A. Global muscle coactivation of the sound limb in gait of people with transfemoral and transtibial amputation. *Sensors* **2020**, *20*, 2543. [CrossRef]
38. Rinaldi, M.; Ranavolo, A.; Conforto, S.; Martino, G.; Draicchio, F.; Conte, C.; Varrecchia, T.; Bini, F.; Casali, C.; Pierelli, F.; et al. Increased lower limb muscle coactivation reduces gait performance and increases metabolic cost in patients with hered-itary spastic paraparesis. *Clin. Biomech.* **2017**, *48*, 63–72. [CrossRef]
39. Demers, L.; Weiss-Lambrou, R.; Ska, B. Development of the Quebec user evaluation of satisfaction with assistive tech-nology (QUEST). *Assist. Technol.* **1996**, *8*, 3–13. [CrossRef]

40. Demers, L.; Weiss-Lambrou, R.; Ska, B. Item analysis of the Quebec user evaluation of satisfaction with assistive tech-nology (QUEST). *Assist. Technol.* **2000**, *12*, 96–105. [CrossRef]
41. England, S.A.; Granata, K.P. The influence of gait speed on local dynamic stability of walking. *Gait Posture* **2007**, *25*, 172–178. [CrossRef]
42. Saini, M.; Kerrigan, D.C.; Thirunarayan, M.A.; Duff-Raffaele, M. The vertical displacement of the center of mass during walking: A comparison of four measurement methods. *J. Biomech. Eng.* **1998**, *120*, 133–139. [CrossRef]
43. Whittle, M.W. Three-dimensional motion of the center of gravity of the body during walking. *Hum. Mov. Sci.* **1997**, *16*, 347–355. [CrossRef]
44. Ilg, W.; Seemann, J.; Giese, M.; Traschütz, A.; Schöls, L.; Timmann, D.; Synofzik, M. Real-life gait assessment in degenerative cerebellar ataxia: Toward ecologically valid biomarkers. *Neurology* **2020**, *95*, e1199–e1210. [CrossRef]
45. Cavagna, G.A.; Thys, H.; Zamboni, A. The sources of external work in level walking and running. *Physiol. J.* **1976**, *262*, 639–657. [CrossRef]
46. Cavagna, G.A.; Willems, P.A.; Legramandi, M.A.; Heglund, N.C. Pendular energy transduction within the step in human walking. *J. Exp. Biol.* **2002**, *205*, 3413–3422. [CrossRef] [PubMed]
47. Barbero, M.; Merletti, R.; Rainoldi, A. *Atlas of Muscle Innervation Zones: Understanding Surface Electromyography and Its Applications*; Springer: New York, NY, USA, 2012. [CrossRef]
48. Hermens, H.J.; Freriks, B.; Disselhorst-Klug, C.; Rau, G. Development of recommendations for SEMG sensors and sensor placement procedures. *J. Electromyogr. Kinesiol.* **2000**, *10*, 361–374. [CrossRef]
49. Serrao, M.; Rinaldi, M.; Ranavolo, A.; Lacquaniti, F.; Martino, G.; Leonardi, L.; Conte, C.; Varrecchia, T.; Draicchio, F.; Coppola, G.; et al. Gait patterns in patients with hereditary spastic paraparesis. *PLoS ONE* **2016**, *11*, e0164623. [CrossRef] [PubMed]
50. Dingwell, J.B.; Marin, L.C. Kinematic variability and local dynamic stability of upper body motions when walking at different speeds. *J. Biomech.* **2006**, *39*, 444–452. [CrossRef]
51. Varrecchia, T.; Rinaldi, M.; Serrao, M.; Draicchio, F.; Conte, C.; Conforto, S.; Schmid, M.; Ranavolo, A. Global lower limb muscle coactivation during walking at different speeds: Relationship between spatio-temporal, kinematic, kinetic, and energetic parameters. *J. Electromyogr. Kinesiol.* **2018**, *43*, 148–157. [CrossRef]
52. Steinwender, G.; Saraph, V.; Scheiber, S.; Zwick, E.B.; Uitz, C.; Hackl, K. Intrasubject repeatability of gait analysis data in normal and spastic children. *Clin. Biomech.* **2000**, *15*, 134–139. [CrossRef]
53. Schniepp, R.; Wuehr, M.; Schlick, C.; Huth, S.; Pradhan, C.; Dieterich, M.; Brandt, T.; Jahn, K. Increased gait variability is associated with the history of falls in patients with cerebellar ataxia. *J. Neurol.* **2014**, *261*, 213–223. [CrossRef]
54. Ilg, W.; Milne, S.; Schmitz-Hübsch, T.; Alcock, L.; Beichert, L.; Bertini, E.; Mohamed Ibrahim, N.; Dawes, H.; Gomez, C.M.; Hanagasi, H.; et al. Quantitative gait and balance outcomes for ataxia trials: Consensus recommendations by the Ataxia Global Ini-tiative Working Group on Digital-Motor Biomarkers. *Cerebellum* **2023**, *23*, 1566–1592. [CrossRef]
55. Kobsar, D.; Charlton, J.M.; Tse, C.T.F.; Esculier, J.-F.; Graffos, A.; Krowchuk, N.M.; Thatcher, D.; Hunt, M.A. Validity and reliability of wearable inertial sensors in healthy adult walking: A systematic review and meta-analysis. *J. Neuroeng. Rehabil.* **2020**, *17*, 62. [CrossRef]
56. Chini, G.; Ranavolo, A.; Draicchio, F.; Casali, C.; Conte, C.; Martino, G.; Leonardi, L.; Padua, L.; Coppola, G.; Pierelli, F.; et al. Local Stability of the Trunk in Patients with Degenerative Cerebellar Ataxia During Walking. *Cerebellum* **2017**, *16*, 26–33. [CrossRef] [PubMed]